This manuscript was accepted by Appl. Phys. Lett. Click here to see the version of record.

High sensitivity characterization of the nonlinear electric susceptibility of a glass ceramic in the microwave range

F. Bergmann,[1,2,a)] M. Letz,[1,2] H. Maune,[3] and G. Jakob[2]

[1)] *SCHOTT AG, Hattenbergstr. 10, 55122 Mainz, Germany*

[2)] *Johannes-Gutenberg-Universitt Mainz, Saarstr. 21, 55122 Mainz, Germany*

[3)] *Technische Universitt Darmstadt, Merkstr. 25, 64283 Darmstadt, Germany*

(Dated: 6 May 2019)

The nonlinear electric susceptibility of a glass ceramic is characterized in the microwave range by measuring intermodulation of two high-power signals. To reach the necessary sensitivity for dielectric nonlinearities, the setup ensures that the measured intermodulation can be ascribed to the material under test while all other intermodulation sources are suppressed. This is achieved by coupling three dielectric resonators in a cut-off waveguide. The third order nonlinearity of the glass ceramic is found to be $\chi_3/\varepsilon_r = (1.6 \pm 0.8) \times 10^{-15}\,\mathrm{m^2/V^2}$ at 950 MHz. The magnitude is comparable to previously measured high-end sintered ceramics. The power of the intermodulation signal as a function of the input power deviates from the simple 3 dB/dB scaling and can be modeled by linear-nonlinear interaction.

Keywords: nonlinear susceptibility, passive intermodulation, glass ceramics, dielectric characterization

[a)] Electronic mail: florian.bergmann@schott.com

This manuscript was accepted by Appl. Phys. Lett. Click here to see the version of record.

The response of an insulating material to an electric field is mostly described by just two parameters: The relative dielectric constant ε_r and the normalized loss $\tan\delta = 1/Q_d$. Both are combined in the complex dielectric function $\varepsilon = (1 - i\ \tan\delta)\varepsilon_r\varepsilon_0$. Methods to measure those two characteristics in the microwave range have been developed and are still improved[1,2]. However, those two parameters only give a full picture for linear responses. At higher electric field amplitudes, all dielectrics reveal nonlinear behavior. Nonlinear responses have been investigated in systems where the nonlinearity is a predominant property, e.g. *ferro*electrics[3,4]. But also *di*electrics show a nonlinear response. This is a well known phenomenon in optics[5–7]. In this frequency range, lasers easily enable high electric field amplitudes, where nonlinear dielectric responses become relevant. Despite of the realization of a continuous-wave maser at room temperature[8], the lack of high-power masers complicates the investigation of high-power phenomena at microwave frequencies. Additionally, in the microwave range the loss is orders of magnitude higher than in optical systems. So even with a hypothetical high-power maser, large power dissipation would give rise to effects being much more relevant than the nonlinear response. However, the development of low loss microwave dielectrics[1,9,10] motivates to take a closer look at the nonlinear dielectric response. This is furthermore supported by a challenge engineers are facing in microwave electronics for applications in telecommunication systems: passive intermodulation (PIM). A nonlinear system produces higher harmonics or, if several frequencies are present, sum and difference frequencies, summarized as intermodulation products. If an intermodulation product falls into another channel, its communication is disturbed. This cross talk is especially critical for two channels of completely different power magnitudes, e.g. transmitting and receiving channels at a cell phone base station. To ensure that intermodulations of two high-power transmitted signals do not interfere with the received signal, the power at an intermodulation frequency is typically required to be 170 dB below the power at the original frequencies[11]. This issue becomes even more critical when considering the upcoming mobile communication standard of the fifth generation (5G), which aims to provide massive data rates to an increasing number of devices. It requires higher frequencies and the efficient use of available frequencies. PIM limits the efficient use. Higher frequencies on the other hand require more accurate designs which can be enabled by glass ceramics due to their higher homogeneity compared to sintered ceramics. There is a broad field of PIM generation mechanisms. They can be divided into contact/surface and bulk material nonlinearities. Dirty or

This manuscript was accepted by Appl. Phys. Lett. Click here to see the version of record.

loose contacts[12] are subject to generating PIM as well as dielectric/conductor interfaces[13]. Bulk nonlinear responses can be divided into conductor and insulator nonlinearities. Conductor nonlinearities can be provoked by voids in the metal[12] or the intrinsic nonlinear resistivity[13]. Insulators like ferroelectrics or ferromagnets show a strong nonlinear behavior while dielectrics are expected to behave very linear[14]. Finally, PIM can be an indirect effect of loss and heat dissipation, known as thermo-electric effect[15]. While nonlinear properties of ferroelectrics are favorable for tunable devices[16,17], usual devices are preferred to behave linearly. One major challenge in mitigating PIM is the differentiation between the sources. A lot of experimental effort is put into isolating the sources and finding qualitative distinctions that identify an effect[15,18]. The setup used to obtain the data presented in this paper isolates the bulk material nonlinear dielectric response. It follows the design by Nishikawa *et al.*[19]. They used the setup to compare the nonlinearity and to develop a low distortion sintered ceramic[20]. With their sintered ceramics, they constructed low cross talk filters for cellular base stations[21].

The polarization $\mathbf{P} = (P_1, P_2, P_3)$ at time t is assumed to depend on the instantaneous value of the electric field $\mathbf{E} = (E_1, E_2, E_3)$ at the same time t only (no memory). This assumption is equivalent to describing a loss- and dispersionless dielectric[7]. Following the model from non-resonant nonlinear optics[7], the polarization is written as a tensor expansion with electric susceptibilities χ:

$$\frac{P_i}{\varepsilon_0} = \sum_j \chi_{ij} E_j + \sum_{jk} \chi_{ijk} E_j E_k + \sum_{jkl} \chi_{ijkl} E_j E_k E_l + ... \tag{1}$$

Here, ε_0 is the electric field constant. For an isotropic system, this relation can be simplified to a scalar equation by imposing centro-symmetry: All off-diagonal elements vanish and the remaining diagonal elements turn out to have the same value. Furthermore, the even order terms vanish due to the field reversal condition $\mathbf{E}(t) \to -\mathbf{E}(t) \overset{!}{\Rightarrow} \mathbf{P}(t) \to -\mathbf{P}(t)$. Equation 1 then becomes:

$$P/\varepsilon_0 = \chi_1 E + \chi_3 E^3 + \chi_5 E^5 + ... \tag{2}$$

This nonlinear relation can also be formulated for the electric flux density D:

$$D = \varepsilon_0 \varepsilon_r E(1 + \alpha E^2 + \beta E^4 + ...) \tag{3}$$

with $\alpha = \chi_3/\varepsilon_r$ and $\beta = \chi_5/\varepsilon_r$. This paper deals with the characterization of the cubic nonlinearity α.

The challenge of measuring dielectric nonlinearities lies in the separation from other nonlinearities. A setup to measure dielectric nonlinearities needs to make sure that the high power is solely applied to the material. This is achieved by exploiting a preferable property of intermodulation products compared to higher harmonics: Intermodulation only takes place where two base frequencies are present. By designing a setup where two frequencies are solely present at a designated part of the setup, any measured intermodulation signal can be attributed to this part. A corresponding setup was designed by Nishikawa *et al.*[19]. Three cylindrical dielectric resonators of the same resonance frequency f_0 are lined up in a

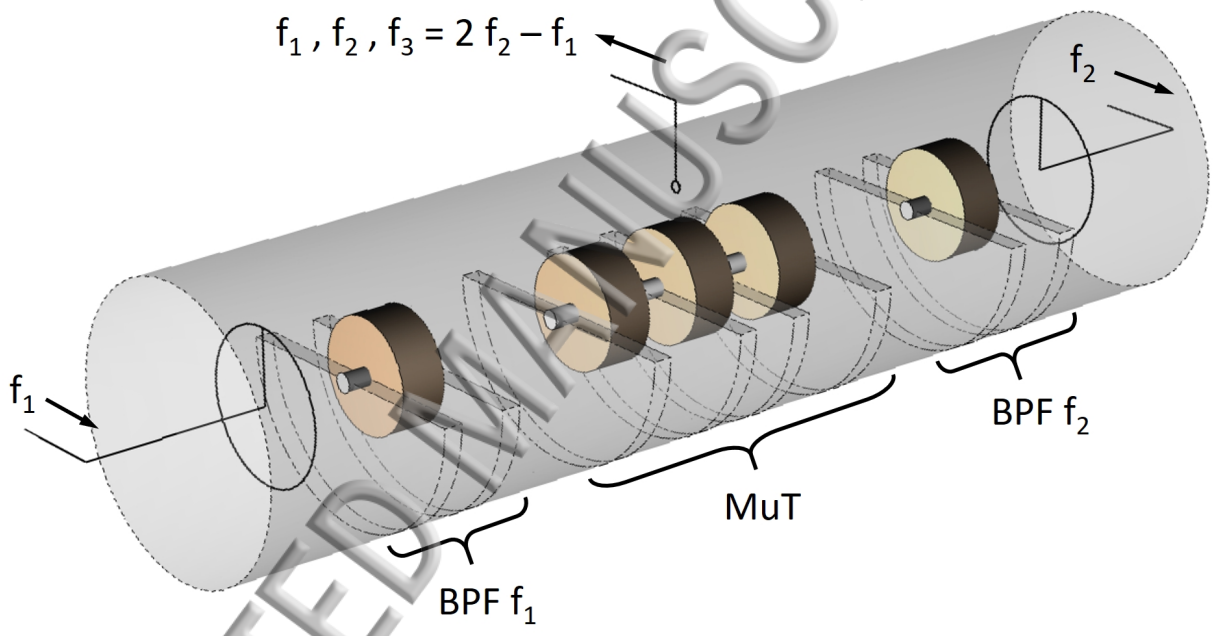

FIG. 1. Sketch of the setup. The three dielectric resonators made of the material under test (MuT) in the center show three resonances following the intermodulation relation $f_3 = 2f_2 - f_1$. The base signals are fed from two different inputs. The loops from magnetic dipoles that excite the $TE_{01\delta}$-mode of the dielectric resonators. The outer dielectric resonators work as filters. The intermodulation signal is picked up above the center resonator.

cut-off waveguide. Assuming weak coupling between next neighbors, the system has three eigenfrequencies f_1, f_2 and f_3 following the relation $f_3 = 2f_2 - f_1$. The frequency relation is equal to the relation for one intermodulation product at frequency f_3 that is generated in a nonlinear system when fed with frequencies f_1 and f_2. Thus, this resonant structure enables

This manuscript was accepted by Appl. Phys. Lett. Click here to see the version of record.

high sensitivity measurements by two manners: First, the field amplitudes of frequencies f_1 and f_2 are enhanced by the Q-factor of the resonance. Second, the intermodulation signal is also enhanced by the Q-factor of the resonance. A sketch of the setup is given in Fig. 3. The material investigated in this work is Poweramic^{TM}GHz33[22], a glass ceramic produced by SCHOTT, which contains $Ba_4Al_2Ti_{10}O_{27}$ as main crystalline phase (mass fraction of 70 %) with crystallites of about 10 µm in diameter. Its linear dielectric properties at 1 GHz are $\varepsilon_r = 32$ and $\tan\delta = 5.5 \times 10^{-4}$. The dielectric resonators have a diameter of 60 mm, an inner drilling of 10 mm and a thickness of 24 mm. The dominant $TE_{01\delta}$-mode of a single dielectric resonator in the cavity has its frequency at $f_0 = 950$ MHz. When the distance between the surfaces of the dielectric resonators is set to 33 mm, the coupled system shows three resonances at $f_1 = 920$ MHz, $f_2 = 950$ MHz and $f_3 = 980$ MHz. The cut-off frequency for the dominant TE_{01}-mode of the cavity is 1172 MHz. The base frequencies are fed into

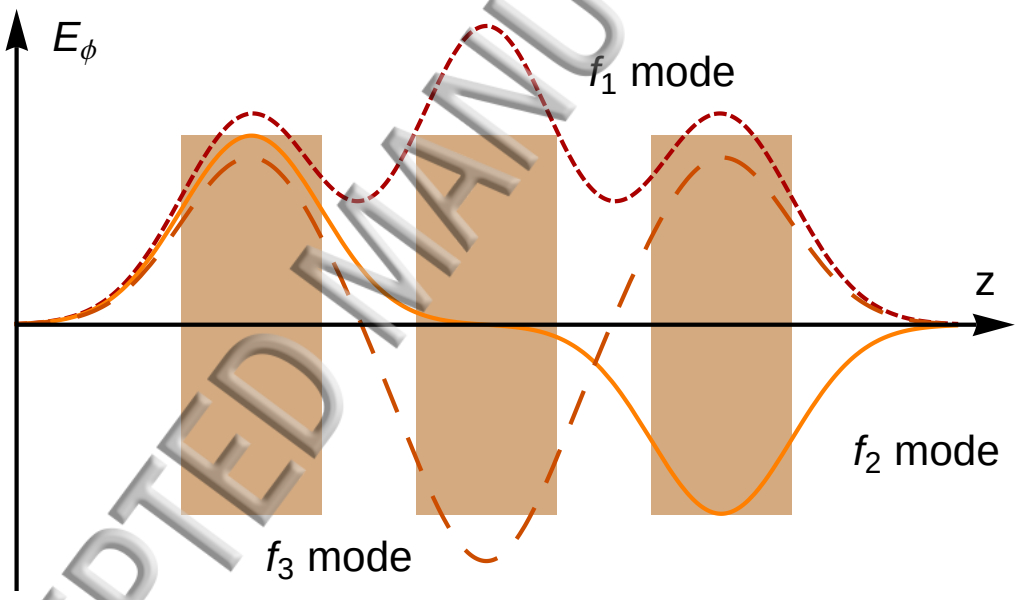

FIG. 2. Sketch of the electric field distribution. The position of the resonators is represented by the rectangles. The second mode has a node at resonator in the center. By placing the output probe above the resonator in the center, intermodulation generation is suppressed in the output system.

the setup from two different inputs, so no intermodulation signal is generated in the input system. To ensure that the signal of the opposite input does not leak into the other input and generated intermodulation, additional resonators are introduced at each input. Their resonances are tuned to the corresponding input frequency. They act as band pass filters

(BPF) with a 3 dB bandwidth of 0.5 MHz. At the output, a loop probe is placed above the

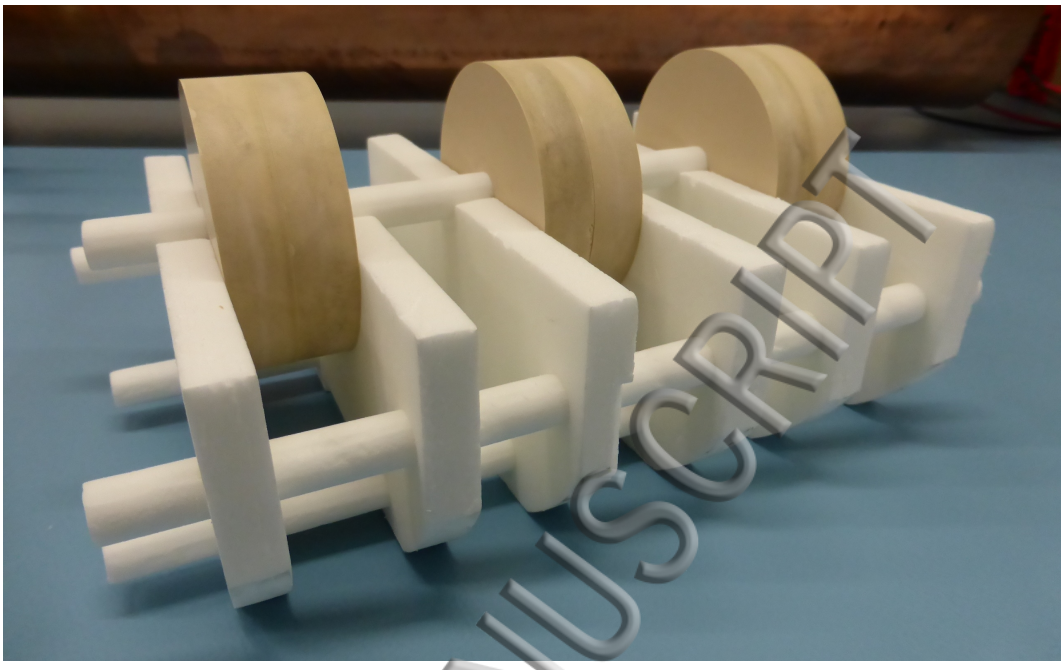

FIG. 3. Three dielectric resonators mounted on the support structure, made of Rohacell® 31 HF. The outer diameter of the dielectric resonators is 60 mm.

center resonator where the power of the second base frequency is much smaller than the one of the first base frequency, due to the node of the second mode at the center resonator. This ensures that no intermodulation happens in the output system. The field distribution of the three modes of the coupled system are sketched in Fig. 2. Before examining the output signal with a spectrum analyzer, a band pass filter for the intermodulation frequency with a 3 dB bandwidth of 10 MHz is used to attenuate the base frequencies to protect the spectrum analyzer but still obtain high sensitivity to the intermodulation signal.

In the actual experimental setup, the largest deviation from this simple model originates from the impossibility to manufacture three resonators of exactly the same resonance frequency. The tolerated relative deviation in frequency directly specifies the relative geometrical tolerance. For the resonators in question the tolerance is 40 µm for a frequency tolerance of 0.5 MHz. The setup is adjusted with a network analyzer (Keysight ENA E5071C). The signals are provided by two signal generators (Keysight MXG N5182A and PSG E8267D). The signal power is amplified by two high power amplifiers (Mini-Circuits ZHL-100W-13+). A tunable BPF (K&L 5BT-500/1000-1-N/N) adjusts the power levels of the output sig-

This manuscript was accepted by Appl. Phys. Lett. Click here to see the version of record.

nal. The adjusted output signal then is scanned with a spectrum analyzer (Keysight MXA N9020A).

The third order nonlinear susceptibility χ_3 is calculated from the relative power levels of f_1 and f_3 at the output and the electric field amplitude of the second frequency f_2 in the resonators, E_2. If an electric field of the form $E(t) = E_1 \sin(\omega_1 t) + E_2 \sin(\omega_2 t)$ is applied to a dielectric described by Equation 3, higher harmonics and intermodulation products are generated. The third order intermodulation signal at $f_3' = 2f_1 - f_2$ is not resonantly enhanced and therefore not detected. However, a certain power P_3 is generated at the intermodulation frequency $f_3 = 2f_2 - f_1$, which feeds the third mode of the coupled system:

$$P_3 = \int \mathrm{d}^3x \left(\frac{3}{4}\alpha(x)E_2^2(x)\right)^2 p_1(x) \tag{4}$$

Here, $p_1(x) = w_1(x)\ \omega_1/2\pi = \varepsilon_0\varepsilon_r(x)E_1^2(x)/4 \times \omega_1/2\pi$ is the time averaged electric power density flowing to location x. At the output the power at f_1 and f_3 are measured. Assuming the impedance of the loop probe to be independent of the frequency, which is a valid assumption for the small relative difference in frequency far from any resonances of the loop, the power ratio corresponds to the energy ratio between the stored energy in the lowest and the higher mode of the coupled resonator system, W_{M1} and W_{M3}.

$$W_{M3} = \frac{Q_3}{2\pi f}\int \mathrm{d}^3x \left(\frac{3}{4}\alpha(x)E_2^2(x)\right)^2 p_1(x) \tag{5}$$

$$W_{M1} = \frac{\varepsilon_0}{4}\int \mathrm{d}^3x\ \varepsilon_r(x)E_1^2(x) \tag{6}$$

The ratio of the power levels is then given by:

$$\frac{W_{M3}}{W_{M1}} = \frac{Q_3}{2\pi}\left(\frac{3}{4}\alpha E_2^2\right)^2 \zeta \tag{7}$$

Here, ζ is a dimensionless number that depends on the field distribution that is obtained in simulations. The electric field amplitude $E_2 = \max[E_2(x)]$ at a given input power is determined from the resonator and coupling properties. Electric field amplitudes of several V/mm are obtained at input powers of 100 W.

One main purpose of the setup is to exclude all intermodulation sources except the nonlinearity of the material. To check whether the setup meets these expectations two tests are performed: First, by introducing the filter resonators, the isolation between the two inputs is at least −60 dB. Additionally, an intermodulation signal generated in the input

This manuscript was accepted by Appl. Phys. Lett. Click here to see the version of record.

system will be attenuated by the filter resonators by 60 dB. This is assumed to suffice to exclude intermodulation generation in the input system. Second, to exclude intermodulation generation in the output, the intermodulation level is compared at different output couplings. It is found that the relative intermodulation level is constant for all output couplings. This implies that the intermodulation is not generated in the output system. It is therefore safe to say that the intermodulation happens in the material only. Fig. 4 shows the output powers of the base frequencies f_1 and f_2 and of the intermodulation frequency $f_3 = 2f_2 - f_1$ for different input powers. Due to the characteristics of the band pass filter

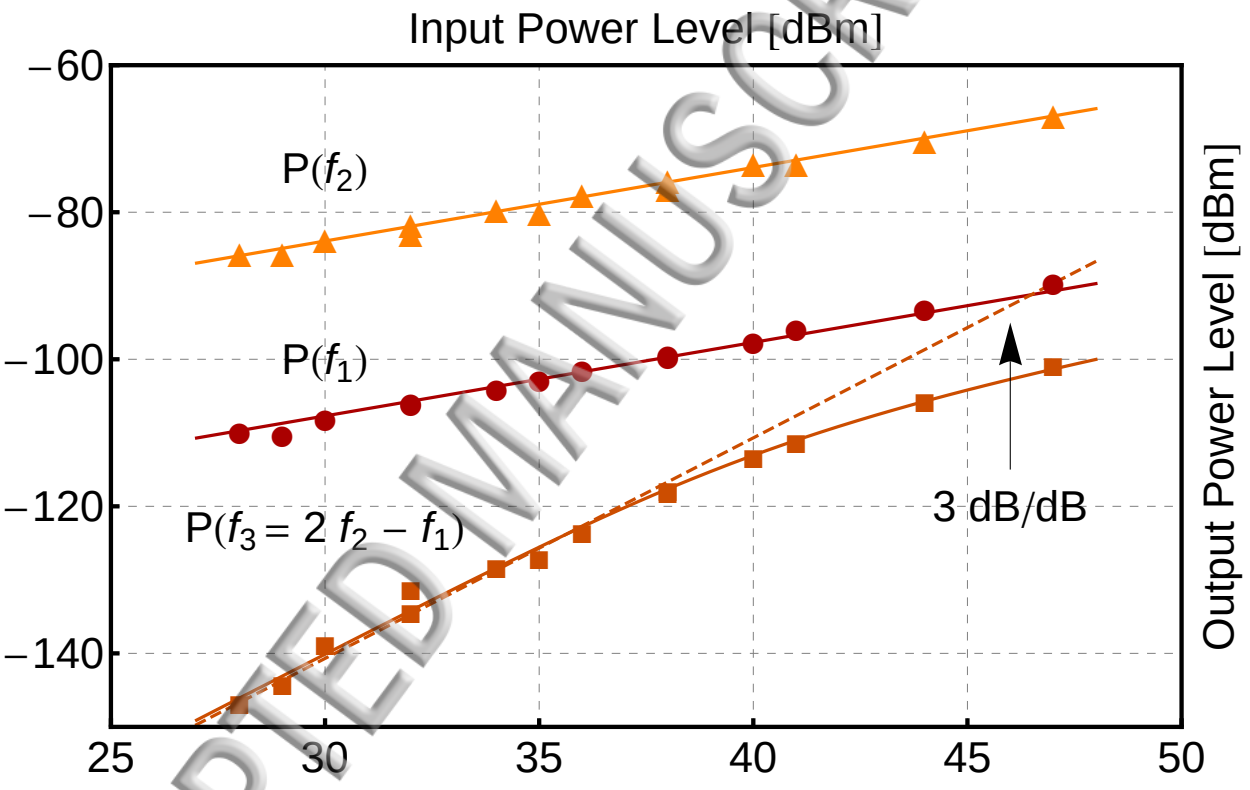

FIG. 4. Measured output powers at frequencies f_1, f_2 and f_3, behind the band pass filter. The power levels of the original frequencies scale 1 dB/dB which is a positive control for the amplifier gain. The intermodulation signal is fitted with the model of a linear-nonlinear interaction as proposed by Henrie *et al.*[23]. For low powers, the intermodulation signal scales with 3 dB/dB.

at the output, the power level at f_2 is attenuated by about 30 dB less than the power at f_1. This is why the power level at f_2 lies above the power level at f_1. For small input powers, the power level at the intermodulation frequency rises with 3 dB/dB. For larger input powers, there is a clear deviation from this trend. Such deviations from a 3 dB/dB

scaling behavior for an third order intermodulation signal have been reported in several other systems. E.g., deviating slopes have been observed in high temperature superconducting microwave devices[24–26] and microstrip lines[27]. The expected 3 dB/dB slope of the intermodulation power originates from the assumption that for the powers in question the transfer function can be appropriately modeled by a third order polynomial. There are several possibilities how this basic assumption may be violated, e.g. higher order terms need to be introduced or even non-analytic transfer functions have been proposed[28]. However, the data is best described with a model by Henrie *et al.*[23,29]. They proposed linear-nonlinear interaction as a cause of non-3 dB/dB scaling. They discuss the nonlinear response of a nonlinear resistance in series with a linear resistance. As depicted in Fig. 4, their model can be used to fit the data. The material nonlinearity α is determined with the data at the low power limit. Four measurement cycles with the same material samples were performed. Between those cycles, the resonator system was destructed and then readjusted. This check for reproducibility yields $\chi_3/\varepsilon_r = (1.6 \pm 0.8) \times 10^{-15}\,\mathrm{m^2/V^2}$. The relative uncertainty of 50 % is the standard deviation of those four measurement cycles. The variation is attributed to differences in setup adjustments and uncertainties in the power levels. The measurements of sintered ceramics by Tamura *et al.*[20] did not observe a deviation from the 3 dB/dB slope. However, their sparse data does not allow to infer significant trends in slope and curvature. Though they do not explicitly state the nonlinearity α of their materials, it is possible to infer the nonlinearity from their given data. Additionally, the attenuation from input to output needs to be guessed for their work. It is about 40 dB for the setup presented in this paper. It is therefore assumed that the attenuation for the corresponding setup by Tamura[20] lies within 30 dB to 60 dB. This estimation gives rise to the error bars plotted in Fig. 5. The nonlinearity of the glass ceramic Poweramic$^{\mathrm{TM}}$GHz33 conforms with the order of magnitude of the nonlinearities measured for high-end sintered ceramics. Tamura *et al.*[20] furthermore suggested that the microwave nonlinearity can be explained by the forth order term in the crystal's Hamiltonian. This approach is analogous to the description in optics[7], where, for non-resonant interaction, the macroscopic model of Equation 1 accurately describes the nonlinear response. Here, electronic polarization gives rise to nonlinear cubic susceptibilities in the order of $\chi_3 = 10^{-22}\,\mathrm{m^2/V^2}$. A simple model of a classical anharmonic oscillator returns the same order of magnitude. At microwave frequencies, by considering optical phonon modes, the nonlinearity shifts to higher values. However, it turns out that

This manuscript was accepted by Appl. Phys. Lett. Click here to see the version of record.

even estimates for very low phonon energies in this simple model do not reach the order of magnitude that was measured. One plausible interpretation of the linear-nonlinear model might be a nonlinear kind of polarization that saturates in combination with another kind of linear polarization.

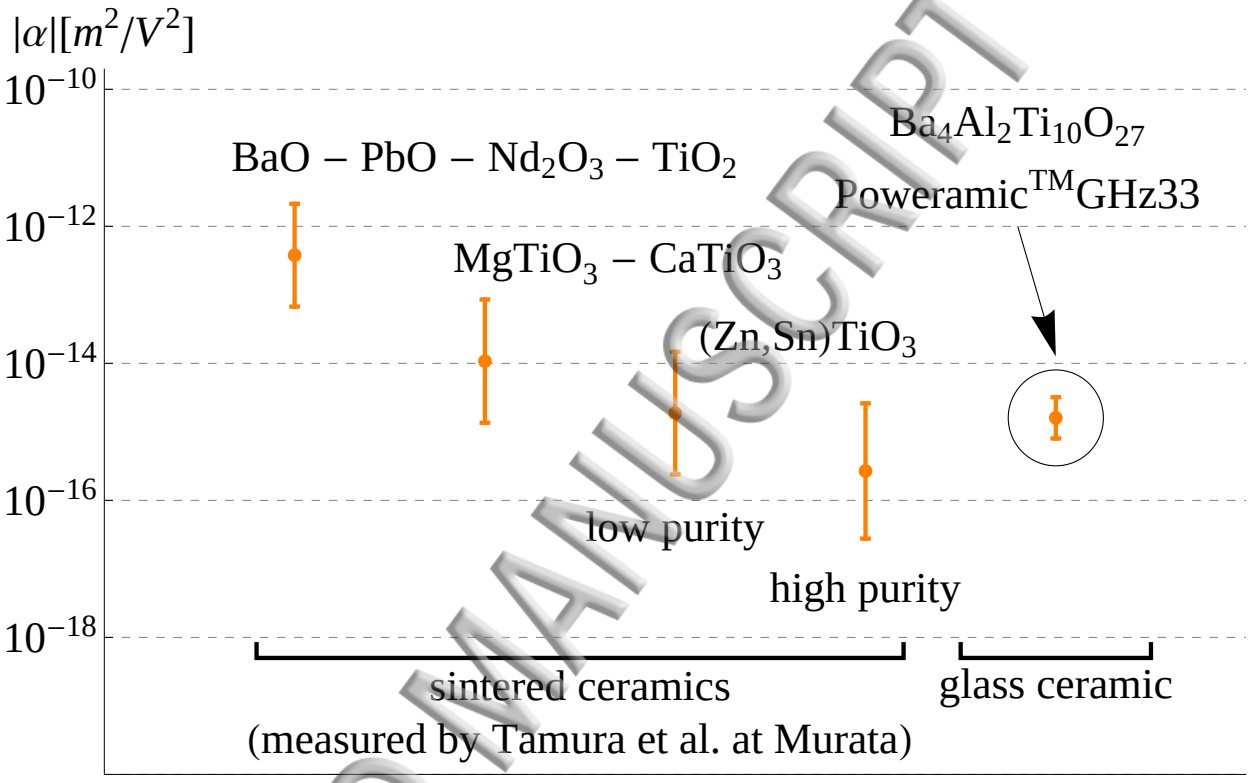

FIG. 5. Comparison of the cubic nonlinearity α of Poweramic™GHz33 with three sintered ceramics measured by Tamura *et al.*[20]. The error bar for the sintered ceramics originates from the need to guess the setup attenuation, which is not given by Tamura *et al.*.

Following the method developed by Nishikawa *et al.*[19], a setup for measuring dielectric nonlinearities in the microwave range was realized. The SCHOTT glass ceramic Poweramic™GHz33 was characterized and shows very small cubic nonlinearity of $\chi_3/\varepsilon_r = (1.6 \pm 0.8) \times 10^{-15}\,\mathrm{m^2/V^2}$. This value is comparable to previously measurements of high-end sintered ceramics. The input power dependence of the intermodulation power can be modeled with linear-nonlinear interaction as done by Henrie *et al.*[23]. This might be due to a saturation of the polarization of one kind in combination with a still linear polarization of another kind. An extension of the present method to characterize further materials is possible.

The authors would like the thank Prof. Rolf Jakoby from the institute of microwave electronics and photonics at the Technische Universitt Darmstadt for the support with the key measurement equipment, and Bernd Porr and Leopold Eichberg from SCHOTT for sample and setup manufacturing.

REFERENCES

[1]M. T. Sebastian and H. Jantunen, International Materials Reviews **53**, 57–90 (2008).

[2]T. Karpisz, B. Salski, P. Kopyt, and J. Krupka, in *2018 IEEE/MTT-S International Microwave Symposium - IMS* (2018) pp. 1397–1400.

[3]L. Curecheriu, S. B. Balmus, M. T. Buscaglia, V. Buscaglia, A. Ianculescu, L. Mitoseriu, and C. A. Randall, Journal of the American Ceramic Society **95**, 3912–3921 (2012).

[4]J. Hemberger, P. Lunkenheimer, R. Viana, R. Böhmer, and A. Loidl, Phys. Rev. B **52**, 13159–13162 (1995).

[5]J. Ballato, M. Cavillon, and P. Dragic, International Journal of Applied Glass Science **9**, 263–277.

[6]R. Adair, L. L. Chase, and S. A. Payne, J. Opt. Soc. Am. B **4**, 875–881 (1987).

[7]R. W. Boyd, *Nonlinear Optics*, third edition ed., edited by R. W. Boyd (Academic Press, Burlington, 2008).

[8]J. Breeze, E. Salvadori, J. Sathian, N. Alford, and C. Kay, Nature **555** (2018).

[9]I. M. Reaney and D. Iddles, Journal of the American Ceramic Society **89**, 2063–2072 (2006).

[10]H. P. Braun, A. Mehmood, M. Hovhannisyan, H. Zhang, D. S. B. Heidary, C. Randall, M. T. Lanagan, R. Jakoby, I. M. Reaney, M. Letz, and H.-J. Elmers, Journal of the European Ceramic Society **37**, 2137 – 2142 (2017).

[11]S. J. Fiedziuszko, I. C. Hunter, T. Itoh, Y. Kobayashi, T. Nishikawa, S. N. Stitzer, and K. Wakino, IEEE Transactions on Microwave Theory and Techniques **50**, 706–720 (2002).

[12]P. Lui, Electronics & Communication Engineering Journal **2**, 109 – 118 (1990).

[13]A. P. Shitvov, D. S. Kozlov, and A. G. Schuchinsky, IEEE Transactions on Microwave Theory and Techniques **66**, 865 – 874 (2018).

[14]G. H. Stauss, Memorandum Report 4233, Ch. 5, 65-82 (Naval Research Laboratory Washington D.C., 1980).

[15]J. Wilkerson, I. Kilgore, K. Gard, and M. Steer, IEEE Transactions on Antennas and Propagation **63**, 474–482 (2015).

[16]C. Schuster, A. Wiens, F. Schmidt, M. Nickel, M. Schüßler, R. Jakoby, and H. Maune, IEEE Transactions on Microwave Theory and Techniques **65**, 4572–4583 (2017).

[17]A. M. Hagerstrom, E. Marksz, C. J. Long, J. C. Booth, and N. D. Orloff, in *2017 90th ARFTG Microwave Measurement Symposium (ARFTG)* (2017) pp. 1–6.

[18]A. Christianson and W. Chappell, in *2009 IEEE MTT-S International Microwave Symposium Digest* (2009) pp. 1301–1304.

[19]T. Nishikawa, Y. Ishikawa, and J. Hattori, IEICE. Jpn. Tech. Rep. **MW88-11**, 39 (1988).

[20]H. Tamura, J. Hattori, T. Nishikawa, and K. Wakino, Japanese Journal of Applied Physics **28**, 2528 (1989).

[21]Y. Ishikawa, H. Tamura, T. Nishikawa, and K. Wakino, Ferroelectrics **135**, 371–383 (1992).

[22]M. Hovhannisyan, M. Letz, and G. Kissl, (2015), US Patent 0018193.

[23]J. Henrie, A. Christianson, and W. J. Chappell, Applied Physics Letters **94**, 114101 (2009).

[24]B. A. Willemsen, K. E. Kihlstrom, and T. Dahm, Applied Physics Letters **74**, 753–755 (1999).

[25]A. V. Velichko, Superconductor Science and Technology **17**, 1 (2004).

[26]M. A. Hein, D. E. Oates, P. J. Hirst, R. G. Humphreys, and A. V. Velichko, Applied Physics Letters **80**, 1007–1009 (2002).

[27]A. Shitvov, D. Zelenchuk, and A. Schuchinsky, in *2009 Loughborough Antennas Propagation Conference* (2009) pp. 177–180.

[28]J. Sombrin, G. Soubercaze-Pun, and I. Albert, in *2013 7th European Conference on Antennas and Propagation (EuCAP)* (2013) pp. 25–28.

[29]J. J. Henrie, A. J. Christianson, and W. J. Chappell, IEEE Transactions on Microwave Theory and Techniques **58**, 1230–1237 (2010).

This manuscript was accepted by Appl. Phys. Lett. Click here to see the version of record.

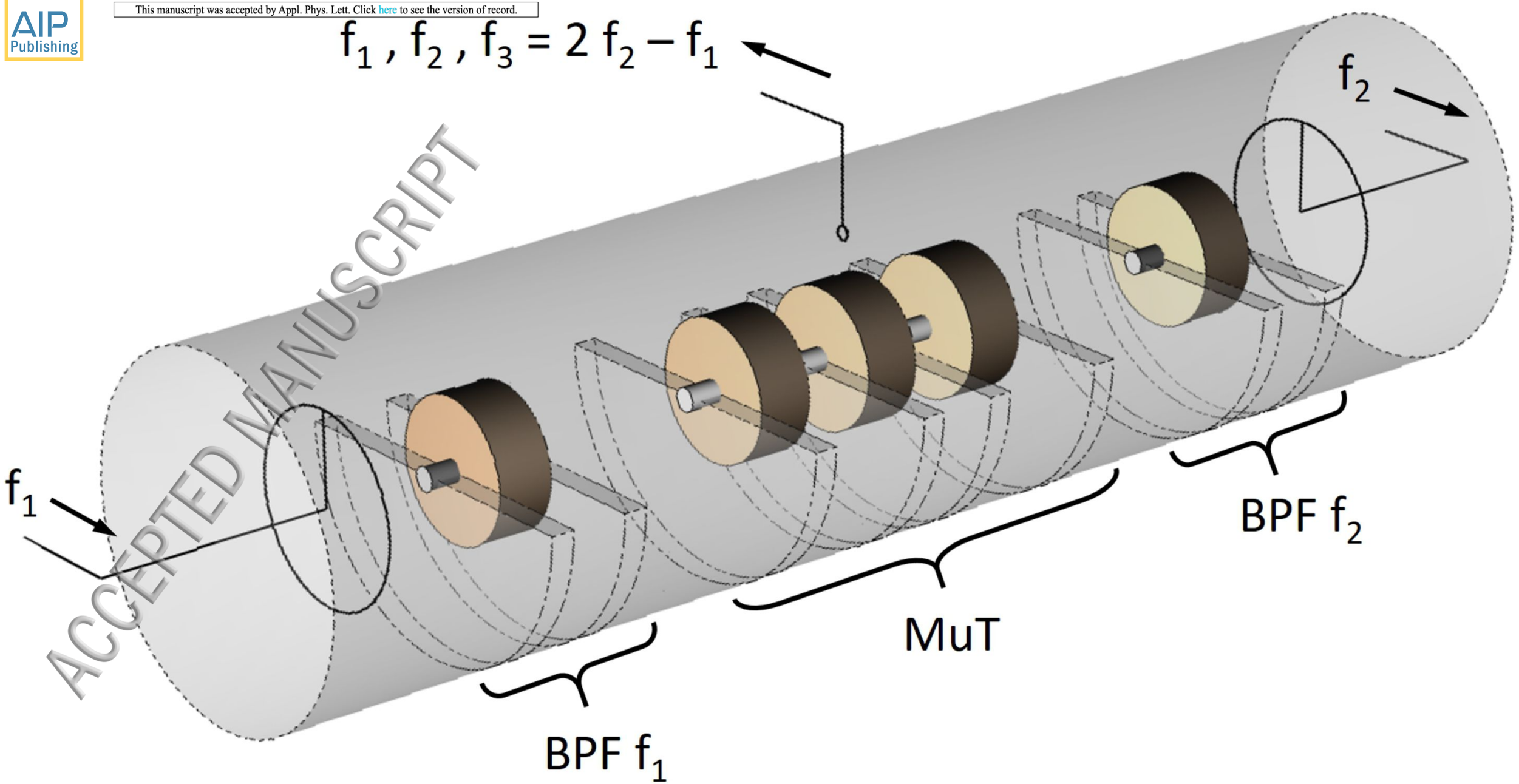

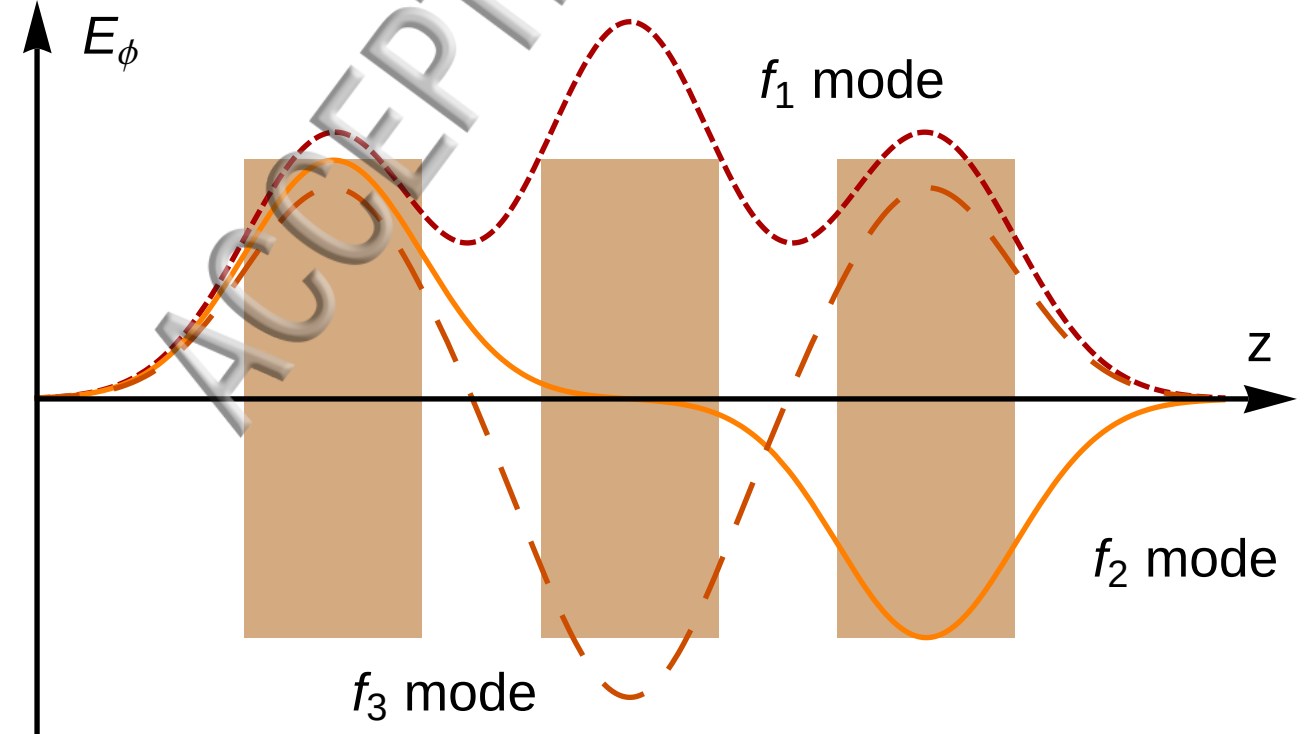
E_ϕ
f_1 mode
z
f_2 mode
f_3 mode

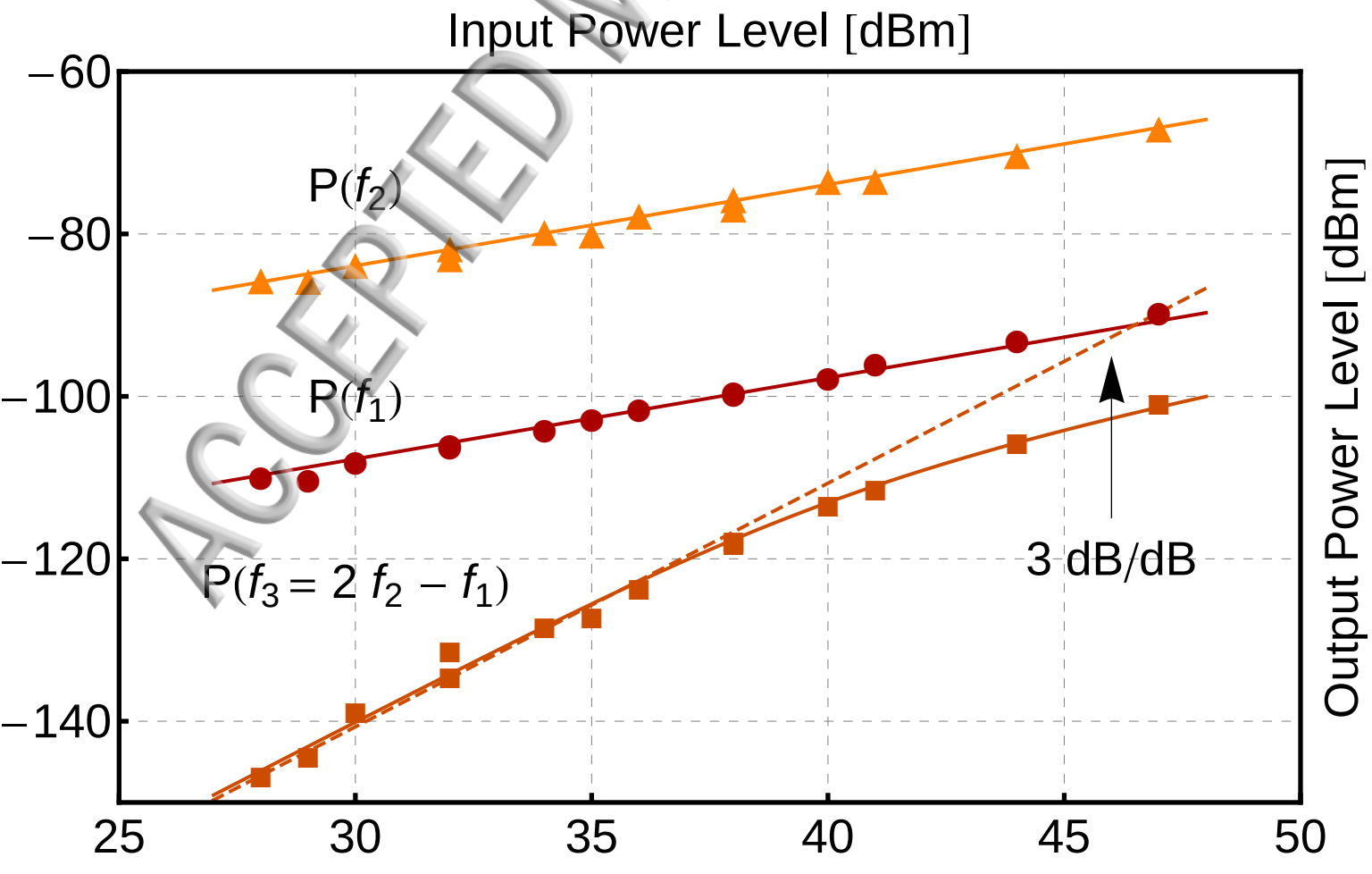
Input Power Level [dBm]
Output Power Level [dBm]
−60
−80
−100
−120
−140
25
30
35
40
45
50
P(f_2)
P(f_1)
P($f_3 = 2\ f_2 - f_1$)
3 dB/dB

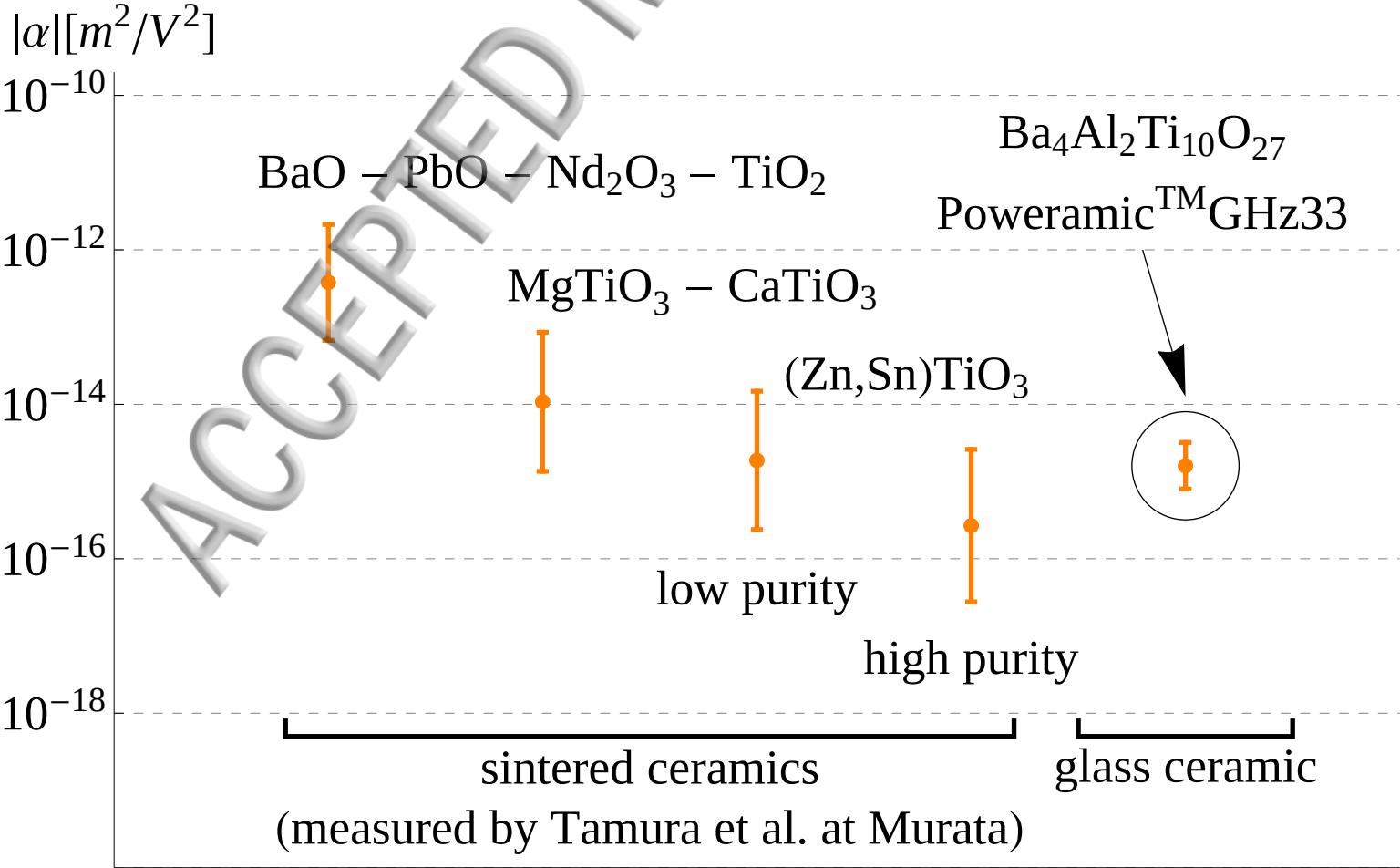
$|\alpha|[m^2/V^2]$
10^{-10}
10^{-12}
10^{-14}
10^{-16}
10^{-18}
$BaO - PbO - Nd_2O_3 - TiO_2$
$MgTiO_3 - CaTiO_3$
$(Zn,Sn)TiO_3$
low purity
high purity
$Ba_4Al_2Ti_{10}O_{27}$
Poweramic™GHz33
sintered ceramics
(measured by Tamura et al. at Murata)
glass ceramic